

lower barrier than the one we are observing in the proton nmr) involves motion of the hydride ligand through the plane of the phosphorus nuclei rendering the carbonyls equivalent but still maintaining the distinction between the two types of phosphorus. Efforts to observe this process using ^{13}C nmr have been unsuccessful.

In summary, although the distinction is not unambiguous, the results tend to favor permutational set II with an exchange intermediate of sufficient concentration to account for the difference between the 90- and 220-MHz spectra. Since it appears that dissociation of one end of a chelate ligand is required for a mechanism consistent with set II, it is possible that the intermediate observed is an "arm off" species.

Acknowledgment. We would like to thank Mr. G. Watunya and Mr. L. J. Rizzardi for obtaining some of the nmr spectra.

Registry No. $\text{TaH}(\text{CO})_2[(\text{CH}_3)_2\text{PCH}_2\text{CH}_2\text{P}(\text{CH}_3)_2]_2$, 50600-13-0.

Supplementary Material Available. A listing of structure factor amplitudes will appear following these pages in the microfilm edition of this volume of the journal. Photocopies of the supplementary material from this paper only or microfiche (105 × 148 mm, 24× reduction, negatives) containing all of the supplementary material for the papers in this issue may be obtained from the Journals Department, American Chemical Society, 1155 16th St., N.W., Washington, D. C. 20036. Remit check or money order for \$3.00 for photocopy or \$2.00 for microfiche, referring to code number INORG-74-1025.

Contribution from the Department of Inorganic Chemistry,
The University of Sydney, N. S. W. 2006, Australia

Evidence for an Intramolecular C-H ··· N Hydrogen Bond in (*E*)-5-Methylpyridine-2-carboxaldehyde-2'-pyridylhydrazone tetracarbonylmolybdenum(0) from Its Crystal Structure and Proton Magnetic Resonance Spectrum

R. St. L. BRUCE, M. K. COOPER,* H. C. FREEMAN, and B. G. McGRATH

Received July 13, 1973

AIC30532N

The crystal structure of (*E*)-5-methylpyridine-2-carboxaldehyde-2'-pyridylhydrazonetetracarbonylmolybdenum(0), $[\text{Mo}(\text{CO})_4(-E)\text{-5-Me}(\text{paphy}) = \text{C}_{16}\text{H}_{12}\text{MoN}_4\text{O}_4]$, has been determined from three-dimensional X-ray data collected by counter methods. The compound crystallizes in space group $P2_1/c$ with $a = 8.326$ (8), $b = 11.916$ (12), $c = 18.056$ (18) Å, $\beta = 93.15$ (10)°, and $Z = 4$. The structure has been refined by full-matrix least-squares techniques to a residual $R = 0.088$ for 1336 independent nonzero reflections. The organic ligand is bidentate. The resulting chelate ring is planar within the limits of precision of the analysis. The octahedral coordination geometry of the metal is slightly distorted. The mean of the M-C bond lengths is 1.99 (2) Å, the Mo-N bond lengths are 2.26 (1) and 2.27 (1) Å, and the N-Mo-N angle is 72.8 (4)°. A short intramolecular contact (C ··· N = 2.85 (2) Å) is interpreted as a C-H ··· N hydrogen bond. Proton magnetic resonance studies show that the short C-H ··· N contact persists in solution and that it therefore cannot be attributed to crystal packing forces.

Introduction

Complexes of molybdenum(0) with the ligands paphy (pyridine-2-carboxaldehyde-2'-pyridylhydrazone), 5-Me(paphy), 5'-Me(paphy), and 5,5'-Me₂paphy exist as pairs of linkage isomers^{1,2} in which the ligand adopts the syn or anti configuration about the carbon-nitrogen double bond. These are bidentate chelate compounds in which the metal is bound to the imine nitrogen and one of the pyridyl nitrogens (Figure 1). Analogous pairs of chromium(0) and tungsten(0) complexes have also been prepared.²

We now report a crystal structure analysis of the linkage isomer in which the ligand 5-Me(paphy) is coordinated to molybdenum(0) in the anti or *E* configuration about the carbon-nitrogen double bond, the methyl group ensuring unambiguous identification of the pyridyl ring bound to the metal. The analysis was carried out to confirm the correctness of the structure of the parent complex $\text{Mo}(\text{CO})_4(-E)\text{-paphy}$ as deduced from the infrared and nmr spectra¹ and to investigate the orientation of the unbound pyridyl ring with respect to the chelating portion of the ligand.

Experimental Section

5-Methylpyridine-2-carboxaldehyde-2'-pyridylhydrazone was prepared by the method of Lions and Martin,³ the intermediate 5-meth-

ylpyridine-2-carboxaldehyde being made according to Ginsburg and Wilson.⁴ The hydrazone was recrystallized from aqueous ethanol. *Anal.* Calcd for $\text{C}_{12}\text{H}_{12}\text{N}_4$: C, 67.9; H, 5.7; N, 26.4. Found: C, 67.6; H, 5.6; N, 26.3.

$\text{Mo}(\text{CO})_4(-E)\text{-5-Me}(\text{paphy})$ was prepared by the reaction of 5-Me(paphy) and the chloropentacarbonylmolybdate(0) anion⁵ at room temperature under a nitrogen atmosphere. Tetraethylammonium chloropentacarbonylmolybdate(0) (1.0 g) was added to a diglyme solution (40 ml) of the ligand (0.5 g). The reaction mixture was stirred for 30 min and filtered to remove the precipitate of tetraethylammonium chloride. Crystallization was induced by the addition of water. After filtering, the complex was washed with ethanol and diisopropyl ether and then stirred with the same solvent for 20 min to remove any molybdenum hexacarbonyl formed as a by-product. The crystals were washed with fresh diisopropyl ether, dried, and stored under nitrogen in the dark. *Anal.* Calcd for $\text{C}_{16}\text{H}_{12}\text{MoN}_4\text{O}_4$: Mo, 22.8; C, 45.7; H, 2.9; N, 13.3. Found: Mo, 23.0; C, 45.7; H, 3.2; N, 13.2.

Crystal Data. $\text{Mo}(\text{CO})_4(-E)\text{-5-Me}(\text{paphy})$ forms small red crystals stable in air and to X-rays at least for the time necessary for data collection. The unit cell is monoclinic with $a = 8.326$ (8), $b = 11.916$ (12), $c = 18.056$ (18) Å, $\beta = 93.15$ (10)°, $U = 1789$ (3) Å³, $d_m = 1.59$ (2) g cm⁻³ (by flotation in an aqueous solution of potassium iodide), and $d_x = 1.56$ (3) g cm⁻³ for $\text{C}_{16}\text{H}_{12}\text{MoN}_4\text{O}_4$, $Z = 4$, with mol wt 420.3. The space group is $P2_1/c$ (No. 14) from systematic absences of reflections ($0k0$ absent for $k = 2n + 1$, $h0l$ absent for $l =$

(3) F. Lions and K. V. Martin, *J. Amer. Chem. Soc.*, **80**, 3858 (1958).

(4) S. Ginsburg and I. B. Wilson, *J. Amer. Chem. Soc.*, **79**, 481 (1957).

(5) E. W. Abel, I. S. Butler, and I. G. Reid, *J. Chem. Soc.*, 2068 (1963).

(1) R. St. L. Bruce, M. K. Cooper, and B. G. McGrath, *Chem. Commun.*, 69 (1970).

(2) M. K. Cooper and B. G. McGrath, unpublished work.

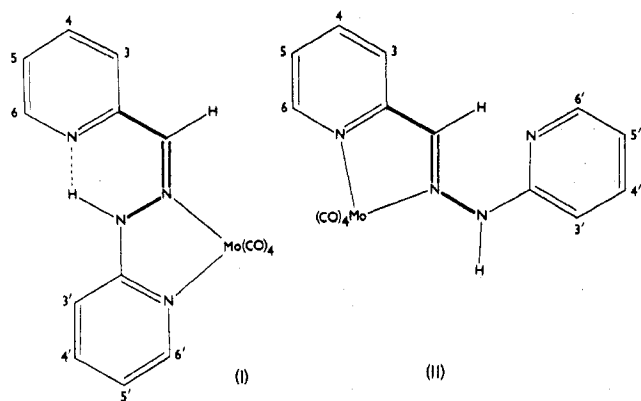


Figure 1. Linkage isomers of Mo(CO)₄paphy. Arabic numerals refer to the hydrogen atoms of the pyridine rings.

$2n + 1$). Accurate reciprocal cell constants were calculated from precise measurements of high-angle reflections from two crystals, using an equininclination diffractometer with Mo K α radiation ($\lambda(\text{Mo K}\alpha)$ 0.7107 Å). The angle β^* was determined from the differences between the ϕ (crystal rotation) angles of several $h00$ and $00l$ reflections.

X-Ray Data Collection. Data were collected at 22° from two crystals mounted about the a and b axes. Intensity measurements were recorded on a fully automated Buerger-Supper equininclination diffractometer⁶ using a scintillation counter (Philips PW 1964/10) and pulse height analyzer (Philips PW4280). Graphite-monochromated Mo K α radiation was provided by a fully stabilized X-ray generator. The angle subtended at the crystal by the counter aperture was increased with increasing μ (in the range 2° 50'–3° 15'). Reflections were measured in the range 3° $\leq T \leq 60^\circ$ for the zones Hkl , HKl ($0 \leq H \leq 5$) and hkl , hKl ($0 \leq K \leq 9$). For a reflection with net count $I = P - (B_1 + B_2)$ the variance from counting statistics alone was $\sigma^2(I) = P + (B_1 + B_2)$, where P is the peak count and B_1 and B_2 are the background counts. The scan range and speed were calculated for each reflection,⁷ the scan speed being such (above a preset minimum) as to make $\sigma(I)/I$ constant. A reflection was considered unobservably weak if the relationship $I \leq 2.8(B_1 + B_2)^{1/2}$ was obeyed.

The unobservably weak reflections were assigned intensities I_{\min} and variances $\sigma^2(I_{\min})$ according to the expressions of Hamilton.⁸ Lorentz-polarization corrections were applied. The dimensions of the crystals used to record data about the a and b axes were respectively $0.10 \times 0.06 \times 0.06$ and $0.05 \times 0.08 \times 0.08$ mm, measured parallel to a , b , and c . Maximum and minimum absorption corrections differed by less than 1.5% in both cases, using standard absorption coefficients⁹ ($\mu(\text{Mo K}\alpha) = 7.53 \text{ cm}^{-1}$). Accordingly the data were not corrected for absorption. The data were merged to a common scale using the method of Rae¹⁰ to give a total of 1336 independent reflections with intensities above the observable threshold.

Solution and Refinement of the Structure. The structure was solved by the use of a sharpened Patterson synthesis and heavy-atom Fourier techniques. In refinement, the function $\Sigma w(|F_o| - s|F_c|)^2$ was minimized by full-matrix least squares using the program ORFLS¹¹ ($w = 1/\sigma^2(F_o)$ is the weight given to each reflection and s is the inverse of the scale factor to be applied to $|F_c|$). Initially, unit weights were assigned to all observed reflections, and zero weights to the unobservably weak reflections. After four cycles in which the overall scale factor, the atomic coordinates, and the isotropic temperature factors were varied, the residuals $R_1 = \Sigma \Delta / \Sigma |F_o|$ and $R_2 = [\Sigma w \Delta^2 / \Sigma w F_o^2]^{1/2}$ were 0.122 and 0.105, respectively ($\Delta = |F_o| - s|F_c|$).

An analysis of $(1/\Delta^2)$ in ranges of $|F_o|$ and $(\sin \theta)/\lambda$ indicated a systematic dependence on both $|F_o|$ and $(\sin \theta)/\lambda$. New weights were calculated for each structure factor using the Cruickshank function¹² $w = (1 - \exp[b(\sin \theta)/\lambda + a^2])/c + d|F_o| + e|F_o|^2 + f|F_o|^3$, and these were modified after each subsequent refinement

(6) H. C. Freeman, J. M. Guss, C. E. Nockolds, R. Page, and A. Webster, *Acta Crystallogr., Sect. A*, **26**, 149 (1970).

(7) H. C. Freeman and I. E. Maxwell, *Inorg. Chem.*, **8**, 1293 (1969).

(8) W. C. Hamilton, *Acta Crystallogr.*, **8**, 185 (1955).

(9) "International Tables for X-Ray Crystallography," Vol. 3, Kynoch Press, Birmingham, England, 1962.

(10) (a) A. D. Rae, *Acta Crystallogr., Sect. A*, **19**, 683 (1965);

(b) A. D. Rae and A. B. Blake, *ibid.*, **20**, 586 (1966).

(11) W. R. Busing, K. O. Martin, and H. A. Levy, Report ORNL-TM-305, Oak Ridge National Laboratory, Oak Ridge, Tenn., 1962.

cycle. The final parameters were $a = -9 \times 10^{-1}$, $b = -4.78 \times 10^{-2}$, $c = 6.32 \times 10^{-2}$, $d = -1.35 \times 10^{-3}$, $e = 8.15 \times 10^{-6}$, and $f = 0$. After three further cycles in which the metal atom and the carbon and oxygen atoms of the carbonyl groups were assigned anisotropic thermal parameters an $(F_o - F_c)$ synthesis showed significant positive electron density in the positions expected for the hydrogen atoms attached to the pyridine rings. Their inclusion caused a decrease in R_1 from 0.090 to 0.088.

The least-squares refinement converged to give residuals $R_1 = 0.088$ and $R_2 = 0.066$. The final value of $\Sigma w \Delta^2 / (m - n)$ was 0.809, where m is the number of independent observations and n is the number of degrees of freedom. The maximum parameter shift in the final cycle was 0.03 standard deviation. A final difference Fourier map had no positive maxima greater than $0.5 \text{ e}/\text{Å}^3$ except in the vicinity of the metal (maximum $0.8 \text{ e}/\text{Å}^3$). All reflections with intensities below the observable threshold had calculated structure amplitudes within three standard deviations $\sigma(F_{\min})$ of their values F_{\min} (see above).

For Mo, C, O, and N the atomic scattering factors used were those given by Cromer and Waber¹³ and for H, those of Stewart, Davidson, and Simpson.¹⁴ The real component of the correction for anomalous dispersion (-1.79 e^{15}) was added to the scattering curve for molybdenum. After the least-squares refinement had converged, the imaginary part of the anomalous dispersion (0.93^{15}) for molybdenum was included in a further cycle. This caused shifts of less than 0.1 standard deviation in the atomic coordinates. All the temperature factors changed by less than 0.2 standard deviation, except those of N(1), N(2), N(3), and N(4) which increased by approximately 1 standard deviation. There was no evidence that the data were affected by extinction. Final positional and thermal parameters are listed in Table I.

Description of the Structure

The bond lengths and angles are shown in Table II and in Figure 2, which also explains the atom-numbering scheme. A stereoscopic view of the molecule is given in Figure 3. The ligand is bidentate, being bound to the metal through the imino and aldehydic pyridyl nitrogen atoms. This confirms the assignment of the donor atoms made on the basis of the nmr and ir spectra of the complex and its parent, Mo(CO)₄-(E)-paphy.¹ The dimensions of the ligand are as expected, with the exception of the angle N(2)-N(3)-C(11) ($128(1)^\circ$). This angle is considerably larger than that expected for an sp^3 nitrogen atom. There is no doubt that a proton is attached to N(3), since this is clearly observed in the nmr spectrum.¹ As the ligand is planar to within 0.1 Å (Table III), we conclude that the hybridization of N(3) is sp^2 , that the lone pair is in an orbital of predominantly p character, and that there is significant electron delocalization over the whole ligand. This is shown also by the short N(2)-N(3) bond. The individual pyridyl rings and the chelate ring are planar within the limits of precision (Table III). The pyridyl rings are inclined at approximately 6° to one another.

The metal lies at the center of a slightly distorted octahedron of donor atoms with metal-carbon and carbon-oxygen bond lengths within the range of values found in similar structures.¹⁶ The metal-ligand bond angle which deviates most from 90° is N(1)-Mo-N(2) ($72.8(4)^\circ$). This is due to the rigid bond angle requirements at C(9) and C(10). The corresponding angle in Mo(CO)₃(bipy)(py) is $72.6(4)^\circ$.¹⁶ An important feature of the structure is the close contact between N(4) and C(10) (2.85(3) Å). On the basis of the X-ray determination and nmr analysis we propose that this contact represents a $\text{CH} \cdots \text{N}$ hydrogen bond. The struc-

(12) J. S. Rollett and O. S. Mills in "Computing Methods and the Phase Problem in X-Ray Crystal Analysis," R. Pepinsky, Ed., Pergamon Press, New York, N. Y., 1961, p 117.

(13) D. T. Cromer and J. T. Waber, *Acta Crystallogr.*, **18**, 104 (1965).

(14) R. F. Stewart, E. R. Davidson, and W. T. Simpson, *J. Chem. Phys.*, **42**, 3175 (1965).

(15) D. T. Cromer, *Acta Crystallogr.*, **18**, 17 (1965).

(16) A. Griffiths, *J. Cryst. Mol. Struct.*, **1**, 75 (1971).

Table I. Fractional Atomic Positional Parameters and Temperature Factors for Mo(CO)₄-(*E*)-5-Me(papy)^{a,b}

Atom	10 ⁴ x	10 ⁴ y	10 ⁴ z	10 ⁴ β ₁₁	10 ⁴ β ₂₂	10 ⁴ β ₃₃	10 ⁴ β ₁₂	10 ⁴ β ₁₃	10 ⁴ β ₂₃
Mo	666 (2)	1695 (1)	1758 (1)	151 (3)	43 (1)	13 (0)	15 (3)	11 (1)	-1 (1)
O(1)	3715 (18)	3273 (16)	2020 (8)	240 (37)	181 (20)	51 (6)	-28 (27)	-1 (1)	-38 (11)
O(2)	2078 (17)	593 (11)	3205 (7)	298 (37)	81 (14)	32 (5)	28 (16)	-25 (11)	8 (7)
O(3)	-1443 (17)	3310 (13)	2672 (6)	370 (36)	81 (12)	30 (5)	29 (23)	41 (11)	-9 (8)
O(4)	-2271 (20)	13 (15)	1873 (9)	346 (47)	156 (21)	58 (8)	-77 (24)	28 (15)	33 (10)
C(1)	2615 (23)	2742 (18)	1889 (9)	109 (43)	127 (24)	18 (6)	28 (25)	-17 (13)	-19 (10)
C(2)	1509 (22)	983 (15)	2647 (9)	177 (41)	78 (18)	14 (6)	50 (23)	-8 (13)	2 (9)
C(3)	-661 (24)	2724 (15)	2338 (9)	251 (51)	53 (17)	14 (6)	28 (23)	-4 (14)	10 (8)
C(4)	-1161 (27)	622 (19)	1799 (10)	241 (57)	125 (26)	14 (7)	28 (30)	26 (16)	26 (11)

Atom	10 ⁴ x	10 ⁴ y	10 ⁴ z	B, Å ²	Atom	10 ⁴ x	10 ⁴ y	10 ⁴ z
N(1)	-101 (14)	2435 (10)	644 (6)	1.7 (3)	H(6)	-1267	3700	1033
N(2)	1824 (14)	651 (10)	884 (6)	1.9 (3)	H(4)	-1167	3383	-1250
N(3)	2812 (15)	-208 (11)	1109 (7)	2.6 (3)	H(3)	600	1917	-983
N(4)	3455 (14)	-951 (10)	-78 (7)	2.5 (3)				
C(5)	-1049 (17)	3351 (16)	526 (7)	3.0 (3)	H(3')	4900	-1300	1550
C(6)	-1482 (19)	3811 (13)	-162 (8)	2.8 (3)	H(4')	5800	-3233	933
C(7)	-867 (18)	3227 (17)	-766 (8)	3.4 (3)	H(5')	5900	-3067	-483
C(8)	111 (18)	2299 (12)	-673 (8)	2.2 (3)	H(6')	4833	-1583	-900
C(9)	485 (15)	1905 (12)	42 (6)	1.5 (3)				
C(10)	1514 (18)	962 (12)	187 (8)	2.2 (3)				
C(11)	3644 (20)	-978 (14)	668 (9)	3.6 (4)				
C(12)	4591 (20)	-1788 (18)	1067 (8)	4.2 (4)				
C(13)	5460 (23)	-2526 (16)	665 (10)	4.8 (5)				
C(14)	5321 (21)	-2504 (14)	-99 (9)	3.8 (4)				
C(15)	4290 (17)	-1733 (17)	-445 (7)	3.1 (3)				
C(16)	-2577 (20)	4817 (14)	-260 (8)	3.5 (4)				

^a Numbers in parentheses are estimated standard deviations. ^b The form of the anisotropic temperature factor T is $T = \exp[-(h^2\beta_{11} + k^2\beta_{22} + l^2\beta_{33} + 2hk\beta_{12} + 2hl\beta_{13} + 2kl\beta_{23})]$.

Table II. Bond Lengths and Angles in Mo(CO)₄-(*E*)-5-Me(papy)^a

Atoms	Distances, Å	Atoms	Distances, Å
Mo-N(1)	2.26 (1)	C(6)-C(7)	1.41 (2)
Mo-N(2)	2.27 (1)	C(7)-C(8)	1.38 (2)
Mo-C(1)	2.05 (2)	C(8)-C(9)	1.39 (2)
Mo-C(2)	1.92 (2)	C(9)-C(10)	1.43 (2)
Mo-C(3)	1.99 (2)	C(11)-C(12)	1.42 (2)
Mo-C(4)	1.99 (2)	C(12)-C(13)	1.37 (2)
N(1)-C(5)	1.36 (2)	C(13)-C(14)	1.38 (2)
N(1)-C(9)	1.37 (1)	C(14)-C(15)	1.38 (2)
N(2)-N(3)	1.36 (2)	C(16)-C(6)	1.51 (2)
N(2)-C(10)	1.32 (2)	C(1)-O(1)	1.13 (2)
N(3)-C(11)	1.42 (2)	C(2)-O(2)	1.18 (2)
N(4)-C(11)	1.35 (2)	C(3)-O(3)	1.15 (2)
N(4)-C(15)	1.36 (2)	C(4)-O(4)	1.19 (2)
C(5)-C(6)	1.39 (2)		

Atoms	Angles, deg	Atoms	Angles, deg
N(1)-Mo-N(2)	72.8 (4)	Mo-C(4)-O(4)	175 (2)
N(1)-Mo-C(1)	92.7 (6)	C(5)-N(1)-C(9)	118 (1)
N(1)-Mo-C(2)	173.5 (6)	N(3)-N(2)-C(10)	125 (1)
N(1)-Mo-C(3)	95.2 (5)	N(2)-N(3)-C(11)	128 (1)
N(1)-Mo-C(4)	96.1 (6)	C(11)-N(4)-C(15)	116 (1)
N(2)-Mo-C(1)	92.8 (6)	N(1)-C(5)-C(6)	125 (1)
N(2)-Mo-C(2)	101.0 (6)	C(5)-C(6)-C(7)	114 (1)
N(2)-Mo-C(3)	167.4 (6)	C(5)-C(6)-C(16)	123 (1)
N(2)-Mo-C(4)	91.7 (6)	C(7)-C(6)-C(16)	123 (1)
C(1)-Mo-C(2)	85.5 (7)	C(6)-C(7)-C(8)	123 (1)
C(1)-Mo-C(3)	91.3 (8)	C(7)-C(8)-C(9)	119 (1)
C(1)-Mo-C(4)	171.0 (7)	N(1)-C(9)-C(8)	121 (1)
C(2)-Mo-C(3)	91.1 (7)	C(8)-C(9)-C(10)	122 (1)
C(2)-Mo-C(4)	86.0 (8)	N(1)-C(9)-C(10)	117 (1)
C(3)-Mo-C(4)	85.9 (8)	N(2)-C(10)-C(9)	119 (1)
Mo-N(1)-C(5)	126.0 (9)	N(3)-C(11)-N(4)	121 (2)
Mo-N(1)-C(9)	115.5 (9)	N(3)-C(11)-C(12)	115 (1)
Mo-N(2)-N(3)	118.5 (8)	N(4)-C(11)-C(12)	124 (2)
Mo-N(2)-C(10)	116 (1)	C(11)-C(12)-C(13)	118 (2)
Mo-C(1)-O(1)	174 (2)	C(12)-C(13)-C(14)	120 (2)
Mo-C(2)-O(2)	176 (2)	C(13)-C(14)-C(15)	119 (2)
Mo-C(3)-O(3)	179 (2)	C(14)-C(15)-N(4)	124 (1)

^a Numbers in parentheses are estimated standard deviations, right-adjusted to the least significant digit of the preceding number.

tural criteria for the existence of such a hydrogen bond are the C...N and H...N distances. Each is required to be

Table III. Least-Squares Planes of Best Fit

(a) Coefficients of the Planes Defined by $AZ + BY + CZ + D = 0$, Where $X = ax + cz \cos \beta$, $Y = by$, and $Z = cz \sin \beta$

No.	Plane	A	B	C	D
I	Hydrazone pyridyl ring	0.7692	0.6388	-0.0157	-1.4960
II	Aldehyde pyridyl ring	-0.8072	-0.5871	-0.0620	1.6581
III	Whole papy ligand	-0.7989	-0.6006	-0.0323	1.7072
IV	Chelate ring	-0.7955	-0.6035	-0.0551	1.6954

(b) Perpendicular Distances of Atoms from Planes, Å

Atom	Plane I	Plane II	Plane III	Plane IV
Mo	(0.04) ^a	(-0.03)	(0.09)	0.00
N(1)	(0.23)	0.00	0.05	0.00
N(2)	(0.07)	(-0.05)	0.05	0.00
N(3)	(0.03)	(-0.12)	0.01	(-0.04)
N(4)	0.00	(0.00)	0.09	(0.09)
C(5)	(0.33)	0.00	0.02	(-0.03)
C(6)	(0.147)	-0.01	-0.04	(-0.06)
C(7)	(0.49)	0.01	-0.04	(-0.04)
C(8)	(0.39)	0.00	-0.03	(-0.02)
C(9)	(0.26)	0.00	0.02	0.00
C(10)	(0.19)	(-0.04)	0.02	0.00
C(11)	0.02	(-0.13)	0.00	(-0.03)
C(12)	-0.03	(-0.21)	-0.05	(-0.08)
C(13)	0.01	(-0.27)	-0.10	(-0.12)
C(14)	0.02	(-0.16)	-0.04	(-0.03)
C(15)	-0.02	(0.00)	0.08	(0.11)
C(16)	(0.55)	(0.03)	-0.03	(-0.06)

(c) Dihedral Angles between Planes

Planes	Angle, deg	Planes	Angle, deg
I, II	5.8	II, III	1.9
I, III	3.9	III, IV	1.3
I, IV	4.8		

^a Distances shown in parentheses refer to atoms *not* included in the calculation of a plane.

shorter than the sum of the van der Waals radii of the atoms involved.¹⁷ The comparisons¹⁸⁻²¹ of Table IV show that the C(10)-H...N(4) interaction fulfills this condition. The hy-

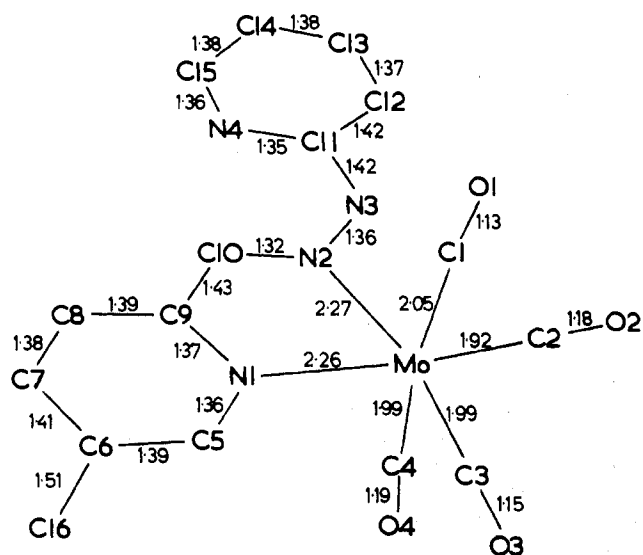
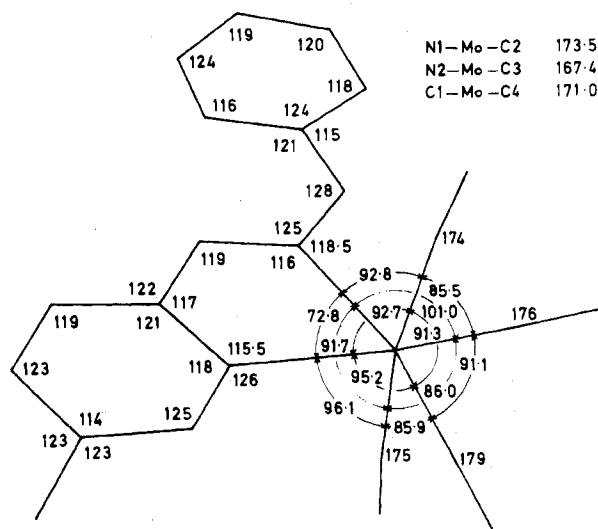
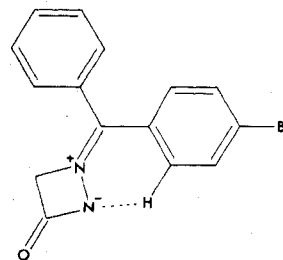
Figure 2. Bond lengths and angles in Mo(CO)₄-(*E*)-5-Me(paphy).Figure 3. Stereoscopic view of Mo(CO)₄-(*E*)-5-Me(paphy).

Table IV

	$d(\text{C} \cdots \text{N})$, Å	$d(\text{H} \cdots \text{N})$, Å
Observed	2.85 (3)	2.1
Sum of normal van der Waals radii ^{18,19,21}	3.2	2.7
Lower limit for nonbonded contacts in peptides ^{20,21}	2.9	2.3

drogen atom attached to C(10) was not located crystallographically. Its position may be inferred by assuming that it lies in the plane defined by N(2), C(9), and C(10), with a C-H bond length of 1.05 Å and a N(2)-C(10)-H angle of 120°. This position leads to the H···N distance shown above. If the hydrogen atom were 2.3 Å from N(4) but still in the plane of the ligand molecule, then the angle N(2)-C(10)-H would have to be *ca.* 130°. Alternatively, the N(2)-C(10)-H angle of 120° could be retained if the C-H bond were *ca.* 30° out of the plane of N(2), C(9), and C(10). These distortions are incompatible with sp² hybridization of

C(10) and are unlikely to occur. The CH···N contact in Mo(CO)₄-(*E*)-5-Me(paphy) therefore satisfies the major criteria currently accepted for distinguishing hydrogen bonds from nonbonding contacts in the solid state. The use of short contact distances alone as criteria for hydrogen bonding in crystalline substances is risky, since short contacts may also be caused by crystal packing forces.^{22,23} Only two other examples of a C-H···N hydrogen bond have been proposed in the literature. In crystalline hydrogen cyanide the N···H contact is 2.2 Å,²⁴ while in an α -1-[(*p*-bromophenyl)phenylmethylene]-3-oxo-1,2-diazetidinium inner salt (formula III)



III

(17) W. C. Hamilton and J. A. Ibers, "Hydrogen Bonding in Solids," W. A. Benjamin, New York, N. Y., 1967, p 15.

(18) L. Pauling, "The Nature of the Chemical Bond," 3rd ed, Cornell University Press, Ithaca, N. Y., 1960.

(19) A. Bondi, *J. Phys. Chem.*, **68**, 441 (1964).

(20) S. J. Leach, G. Nemethy, and H. A. Sheraga, *Biopolymers*, **4**, 369 (1966).

(21) The distinction between N(4) and C(12), related by a 180° rotation about the N(3)-C(11) bond, was made on the basis of bond lengths and the mutual consistency of the isotropic thermal parameters of the ring atoms (Table I and Table II).

(22) J. Donohue in "Structural Chemistry and Molecular Biology," A. Rich and N. Davidson, Ed., W. H. Freeman, San Francisco, Calif., 1968, p 459.

(23) T. M. Gorrie and N. F. Haley, *J. Chem. Soc., Chem. Commun.*, 1081 (1972).

(24) W. J. Dulmage and W. N. Lipscomb, *Acta Crystallogr.*, **4**, 330 (1951).

the intramolecular hydrogen bond has an $N \cdots H$ contact of 2.15 Å.²⁵ With respect to the latter, Fritchie and Wells²⁵ argued that the $N \cdots H$ contact was too short to be called anything other than a hydrogen bond. They rejected the hypothesis that the very short contact was the result of the molecule's need to remain planar in order to preserve its electronic delocalization energy.

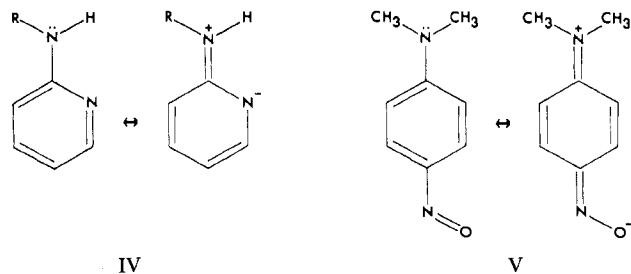
In the case of III, both nmr and infrared spectroscopic data have been cited as evidence for the proposed $C-H \cdots N$ hydrogen bond. The crystallographic authors themselves recorded the nmr spectrum of the unbrominated analog of III. The downfield shift of two (rather than one) of the ten aromatic protons showed that the hydrogen bond was relatively weak. An infrared spectroscopic study of III and several derivatives was carried out by Gorrie and Haley.²³ They recorded the C-H stretching region of these compounds (CCl₄ solution, KBr disk). Pronounced frequency shifts were absent both in solution and in the solid phase. Band intensification was slight and occurred only in the solid phase. It was concluded that the short $C-H \cdots N$ distance in the crystal structure of III was "evidently due to factors other than hydrogen bonding, e.g., crystal packing forces."

The conclusions drawn from both sets of spectroscopic data for III are open to question. The downfield shifts cited by Fritchie and Wells are more likely to arise from the magnetic anisotropy of the $C=N$ group than from other causes.²³ The infrared spectrum of III is highly complex in the C-H stretching region and we question whether the conclusions drawn by Gorrie and Haley are valid.

The preceding arguments are relevant to the present case. We have recorded the nmr spectra of $Mo(CO)_4(E)-5-Me(paphy)$ and a number of closely related molecules. These spectra support our contention that the $C-H \cdots N$ bond in this compound is real, is not caused by crystal packing forces, and persists in solution. In complexes of the type $M(CO)_4(E)-L$, where $M = Cr, Mo, \text{ or } W$ and $L = paphy, 5-Me(paphy), 5'-Me(paphy), \text{ and } 5,5'-Me_2paphy$,²⁶ the chemical shifts of the aldehydic protons are moved well downfield (+1.74 to +2.08 ppm) relative to the free (*E*)-ligand. The deshielding effect of the ring current of the hydrazine pyridine on the aldehyde proton is a maximum when this ring is coplanar with the remainder of the ligand. This maximum value is calculated to be +0.84 ppm,²⁶ using structural parameters obtained from the present work. An additional minor deshielding influence on the aldehydic protons in the *E* complexes arises from coordination. This is most likely less than 0.2 ppm by comparison with the shifts in the protons of the coordinated pyridine ring²⁶ (see Figure 4).

The combined influence of the above two effects leaves a downfield shift of approximately 0.7–1.0 ppm unaccounted for in complex formation. This difference can be explained only if the hydrazine pyridine nitrogen points in the direction of the aldehydic proton, and the hydrazine ring is in the plane of the rest of the ligand. The structure of the complex is then essentially the same in solution as in the solid state, and therefore the short $C-H \cdots N$ distance in the solid cannot be attributed to crystal packing forces.

The orientation of the hydrazine pyridine nitrogen toward the aldehydic proton does not automatically lead to the formation of a $C-H \cdots N$ hydrogen bond. An alternative explanation is illustrated in formula IV, which represents the hydrazine portion of the paphy ligand. It is possible that electron delocalization favors a planar structure so strongly



that there is a barrier to rotation about the $RHN-Ar$ bond. We may deduce the magnitude of this effect in IV by analogy with the energy barrier to rotation in the dimethylamino group of *p*-nitrosodimethylaniline (V). The double-bond character and rotational energy barrier of the R_2N-Ar bond in V should be similar to those of the corresponding bond in IV, since both types of molecules contain strongly electron-donating and -withdrawing groups either ortho or para to each other.

The internal rotation of the dimethylamino group in V has been studied by ¹H nmr spectroscopy^{27,28} and persists to very low temperatures. At room temperature the 100-MHz spectrum of V in CD₂Cl₂ shows a sharp singlet arising from the two methyl groups which experience an averaged magnetic environment because of the rapid rotation about the $Ar-NMe_2$ and $Ar-NO$ bonds.²⁷ At -60° , the rotation of the NMe_2 group is still sufficiently rapid to produce a single resonance for the methyl groups. The proton resonance due to the dimethylamino group is noticeably broadened at -65° , and at -90° it is resolved into two peaks corresponding to the two methyl groups, now nonequivalent by virtue of their asymmetric magnetic environment with respect to the nitroso group.²⁷ The low temperature (-90°) required to stop the rotation of the dimethylamino group in *p*-nitrosodimethylaniline on the nmr time scale suggests that, at room temperature, the rotational energy barrier about the $N(3)-C(11)$ bond is not the major cause of the coplanarity of the hydrazine pyridine ring and the rest of the ligand.

We therefore have strong evidence that there is a significant attractive interaction between the aldehydic proton and the hydrazine pyridine nitrogen in the $M(CO)_4(E)-L$ series of complexes.

Further confirmation of the origin of the large downfield coordination shifts of the aldehydic protons in the *E* complexes is provided by a comparison of the proton shifts of $Mo(CO)_4(E)-5'-Me(paphy)$ and $Mo(CO)_4(E)-paphy$ (*paphy* = pyridine-2-carboxaldehyde-*p*-tolylhydrazine) (Figure 4). The shifts of H(3) and the aldehydic protons in $Mo(CO)_4(E)-5'-Me(paphy)$ are considerably downfield compared to their positions in $Mo(CO)_4(E)-paphy$. This can be explained only if the tolyl group in the latter complex is bent out of the plane of the rest of the ligand. In fact, molecular models imply that it is not sterically possible for the tolyl ring to be in the plane of the rest of the ligand.

Conclusion

The results of the crystal structure determination show clearly that in $Mo(CO)_4(E)-5-Me(paphy)$ the aldehydic proton and N(4) are considerably closer than the sum of the van der Waals radii of hydrogen and nitrogen. From the nmr spectra of this complex and other complexes of the type $M(CO)_4(E)-L$ (where $M = Cr, Mo, \text{ or } W$ and $(E)-L =$

(25) C. J. Fritchie and J. L. Wells, *Chem. Commun.*, 917 (1968).

(26) B. G. McGrath, Ph.D. Thesis, University of Sydney, 1973.

(27) D. D. MacNicol, *Chem. Commun.*, 1516 (1969).

(28) R. K. MacKenzie and D. D. MacNicol, *Chem. Commun.*, 1299 (1970).

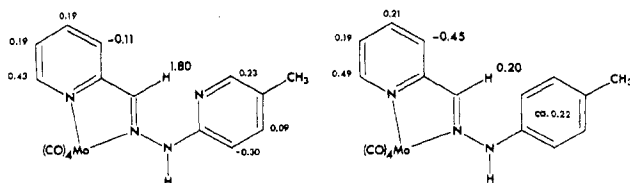


Figure 4. Proton magnetic resonance shifts in $\text{Mo}(\text{CO})_4$ -(*E*)-5'-Me-(paphy) and $\text{Mo}(\text{CO})_4$ -(*E*)-paphy with respect to the free ligand; shifts in ppm positive for increasing δ .

paphy, 5-Me(paphy), 5'-Me(paphy), and 5,5'-Me₂paphy),²⁶ there is strong evidence to show that in solution the chelated ligand remains planar with the lone pair of N(4) directed toward the proton attached to C(10). The large downfield shift of the resonance of this proton on complex formation is consistent with electron drain to N(4) and the formation of a C-H...N hydrogen bond.

Acknowledgment. This work was supported by research grants from the University of Sydney, the Australian Research Grants Committee (Grants 65/15487 and 65/15552), and by two Commonwealth postgraduate studentships (R. St. L. B. and B. G. M.).

Registry No. Tetraethylammonium chloropentacarbonyl-molybdate(0), 14780-96-2; (*E*)-5-methylpyridine-2-carboxaldehyde-2'-pyridylhydrazonetetracarbonylmolybdenum(0), 50830-74-5.

Supplementary Material Available. A listing of structure factor amplitudes will appear following these pages in the microfilm edition of this volume of the journal. Photocopies of the supplementary material from this paper only or microfiche (105 × 148 mm, 24X reduction, negatives) containing all of the supplementary material for the papers in this issue may be obtained from the Journals Department, American Chemical Society, 1155 16th St., N.W. Washington, D. C. 20036. Remit check or money order for \$5.00 for photocopy or \$2.00 for microfiche, referring to code number INORG-74-1032.

Contribution from the Department of Chemistry,
University of Cincinnati, Cincinnati, Ohio 45221

Molecular Structure of Tri(cyclopentadienylmanganese) Tetranitrosyl

R. C. ELDER

Received August 4, 1973

AIC30758Q

The molecular structure of tri(cyclopentadienylmanganese) tetranitrosyl, $(\eta^5\text{-C}_5\text{H}_5)_3\text{Mn}_3(\mu_3\text{-NO})(\mu_2\text{-NO})_3$, has been determined using a Syntex PI X-ray diffractometer. The compound crystallizes in a monoclinic cell, $a = 13.341$ (4), $b = 7.951$ (2), $c = 16.837$ (7) Å, $\beta = 107.73$ (3)°; space group, $P2_1/c$; $Z = 4$. Least-squares refinement using anisotropic thermal parameters and calculated hydrogen atom positions converged to $wR = 0.012$ and $R = 0.032$. The molecular structure of C_{3v} symmetry consists of an equilateral triangle of metal atoms triply bridged by a nitrosyl above the metal plane and doubly bridged by three nitrosyls along the edges of the metal triangle below the plane. The cyclopentadienyl rings are located off the apices of the metal triangle. The average Mn-Mn bond length is 2.506 (3) Å. The NO bond length increases from doubly bridging, $\mu_2\text{-NO}$, 1.212 (6) to triply bridging nitrosyl, $\mu_3\text{-NO}$, 1.247 (5) Å.

Introduction

Several years ago, a fragmentary account of the structure of tri(cyclopentadienylmanganese) tetranitrosyl, $(\eta^5\text{-C}_5\text{H}_5)_3\text{Mn}_3(\mu_3\text{-NO})(\mu_2\text{-NO})_3$ was communicated,¹ describing a triangular metal atom cluster containing a triply bridging and three doubly bridging nitrosyl groups. The solution of the structure was complicated by an apparent disorder problem. Since that time, Professor Dahl and coworkers at the University of Wisconsin have investigated several analogous structures,^{2,3} viz., $[(\eta^5\text{-C}_5\text{H}_5)_3\text{Mo}_3(\mu_3\text{-S})(\mu_2\text{-S})_3]^+ [\text{Sn}(\text{CH}_3)_3\text{Cl}_2]^-$, in which the sulfur atoms of the cation replace the nitrosyl groups in the manganese compound, and $[(\eta^5\text{-C}_5\text{H}_5)_2\text{Ni}]_2\text{Fe}(\text{CO})_3(\mu_3\text{-CO})_2$, which contains two triply bridging carbonyl moieties, one above and one below the plane of the three metal atoms, and no doubly bridging carbonyls. In solving this structure using Patterson methods, Dr. Teo first found an apparent disorder analogous to that found for the manganese structure; however, a second, direct methods solution led to an ordered structure which was refined without subsequent difficulty. Therefore, Teo and Dahl suggested that perhaps the manganese structure was not truly dis-

ordered. On the basis of this suggestion, the data for the manganese compound have been recollected and the structure solved by direct methods without any evidence of disorder. Since no other triply bridging nitrosyl groups have been reported in the intervening period and due to the interesting nature of the compound its full structure is reported here.

Experimental Section

Preliminary Crystal Data. Needle shaped crystals of $(\eta^5\text{-C}_5\text{H}_5)_3\text{Mn}_3(\mu_3\text{-NO})(\mu_2\text{-NO})_3$ were selected from the material prepared by Dr. Schunn¹ of Du Pont and recrystallized several years ago. Most of these were twinned; however, one single crystal was obtained and used for both precession photographs and intensity measurements. This crystal which appeared black in reflected light was of approximate dimensions 0.1 × 0.1 × 0.3 mm. It was mounted on a glass fiber along the long dimension of the crystal. Preliminary precession photographs of $hk0$, $hk1$, $hk2$, $0kl$, and $1kl$ zones (using Cu K α radiation) showed systematic absences of $h0l$ for l odd and $0k0$ for k odd confirming the original choice of the space group as $P2_1/c$, No. 14.⁴ The approximate cell constants were in agreement with those previously reported¹ ($a = 13.34$, $b = 7.95$, $c = 16.82$ Å, $\beta = 107.8^\circ$) and confirmed the identity of this crystal with the previously studied material. The crystal was placed on a Syntex PI automated diffractometer and optically centered for data collection. Fourteen reflections which were found on a rotation photograph were precisely centered using manufacturer supplied software.⁵ Least-squares

(1) R. C. Elder, F. A. Cotton, and R. A. Schunn, *J. Amer. Chem. Soc.*, **89**, 3645 (1967).

(2) P. J. Vergamini, H. Vahrenkamp, and L. F. Dahl, *J. Amer. Chem. Soc.*, **93**, 6327 (1971).

(3) B. K. Teo, Ph.D. Thesis, University of Wisconsin, Madison, Wis., 1973.

(4) "International Tables for X-Ray Crystallography," Vol. 1, 2nd ed, Kynoch Press, Birmingham, England, 1965.

(5) R. A. Sparks, et al., "Operations Manual Syntex PI Diffractometer," Syntex Analytical Instruments, Cupertino, Calif., 1970.